Coordination Chemistry Reviews, 64 (1985) 1—19
Elsevier Science Publishers B.V., Amsterdam — Printed in The Netherlands

LASER PHOTOLYSIS STUDY ON THE PHOTOSUBSTITUTION IN DIMANGANESE AND DIRHENIUM DECACARBONYLS

T. KOBAYASHI,[1] K. YASUFUKU,[2] J. IWAI,[1] H. YESAKA,[2] H. NODA,[2] AND H. OHTANI[1,*]

[1]Dept. of Physics, Univ. of Tokyo, Bunkyo, Tokyo 113 (Japan)

[2]Inst. of Phys. and Chem. Res., Wako, Saitama 351 (Japan)

ABSTRACT

Two photoprimary processes, (1) the metal-metal bond cleavage to give $M(CO)_5$ and (2) CO dissociation without metal-metal bond cleavage to give coordinately unsaturated dimetallic species, $M_2(CO)_9$, are verified by the laser flash photolysis of $M_2(CO)_{10}$ (M=Mn, Re). The nature of the new species is discussed from the excitation wavelength effect and the quenching experiments with alkyl cyanides for M=Mn, and CO and CCl_4 for M=Mn, Re. Photoreaction of $Mn_2(CO)_9$ is investigated by nanosecond time-resolved double-flash method.

INTRODUCTION

Photoexcitation of all the metal-metal bonded carbonyl compounds has been interpreted consistently by invoking the preferential homolysis of the metal-metal bonds (ref.1). $Mn_2(CO)_{10}$ was considered as a prototypical molecule (ref.2) that embodies the prediction from its simplified molecular orbital diagram (ref.3); the electronic spectrum shows two low-lying absorption features. A low-energy shoulder at 375 nm and an intense band at 336 nm have been assigned to the $d\pi$-σ^* and the σ-σ^* transitions, respectively (ref.4). A more intense band with higher energy at 266 nm is assigned to the d-CO π^* transition. Both of the low-energy transitions populate an excited electron to the metal-metal antibonding σ^* orbital yielding an excited state with zero net bonding between the two metal centers, which should result in the rupture of the Mn-Mn bond to produce the 17-electron $\cdot Mn(CO)_5$ species solely ([process 1]).

$$(OC)_5Mn\text{-}Mn(CO)_5 \xrightarrow{h\nu} 2\cdot Mn(CO)_5 \qquad [1]$$

$$(OC)_5Mn\text{-}Mn(CO)_5 \xrightarrow{h\nu} Mn_2(CO)_9 + CO \qquad [2]$$

Recent results, however, indicate that other primary photoprocesses are also important in accounting for the photochemistry of these metal-metal bonded

*Present address: Hamamatsu Photonics K.K., Hamamatsu, Shizuoka 435 (Japan)

0010-8545/85/$06.65

compounds (ref.5). One example, of which the contribution of a non-homolytic pathway resulting in a second intermediate has been proposed (refs.6-8), is $(C_5H_5)_2Fe_2(CO)_4$. $Mn_2(CO)_{10}$ is the other of which the second primary photoprocess, the dissociation of CO without metal-metal bond cleavage to produce a dimetal species (process [2]), has been fully characterized in solution (refs.9-11) and in low-temperature matrix (ref.12).

In this article, we wish to describe the photochemical features of $Mn_2(CO)_{10}$ in hydrocarbon solution and discuss the importance of the CO dissociation process [2]. Some preliminary views on $Re_2(CO)_{10}$ showing the existence of the similar process besides the homolytic process are included.

Furthermore double-flash experiment on $Mn_2(CO)_{10}$ in cyclohexane was performed to clarify the photochemistry of the ligand-unsaturated intermediate, $Mn_2(CO)_9$, which has an unsymmetrically bridging CO (refs.10,12). The first flash (355 nm, 5 ns FWHM) was used to form $Mn_2(CO)_9$ and $\cdot Mn(CO)_5$ and the second flash (532 nm, 20 ns FWHM) was used to excite $Mn_2(CO)_9$.

METHODS

Materials

$Mn_2(CO)_{10}$ was synthesized by the method described in literature (ref.13) and purified by sublimation. $Mn_2(CO)_9(MeCN)$ and $Mn_2(CO)_9(EtCN)$ were synthesized by Koelle's method (ref.14). The IR spectra of the compounds are in good agreement with those in literature (refs.14,15). The UV spectrum of $Mn_2(CO)_9(MeCN)$ in cyclohexane has maximum at 350 nm and a shoulder at 413 nm and that of $Mn_2(CO)_9(EtCN)$ has maximum at 345 nm and a shoulder at 415 nm. Propionitrile and tributylphosphine were purified by following procedures in literature (refs.16,17). 2-Isocyano-2-methylpropane was prepared by the method of Ugi and Mayr (ref.18) and was fractioned with gas chromatograph. Carbon tetrachloride was treated with sodium carbonate solution, washed with water, dried over calcium chloride, and then distilled under nitrogen atmosphere. Chloroform was washed with concentrated sulfuric acid, sodium carbonate solution, and water. It was dried over calcium chloride and then distilled under nitrogen. Cyclohexane (Merck; Uvasol for fluorometry) and acetonitrile (Wako Pure Chemical; Spectro grade) were used without further purification.

Sample solutions were prepared in vacuo. Solvent stored on K-Na alloy was added in the sample compartment after measuring its volume and the sample cells were hermetically sealed. Then, CO or Ar gas was admitted into them through a side arm with a teflon stop cock.

Nanosecond Spectroscopy

Figure 1 shows the block diagram of nanosecond time-resolved absorption spectroscopy used in the present study. The excitation light sources (LASER 1)

were a N_2 laser (Molectron UV24; 337 nm 10-ns FWHM), a third harmonic (355 nm, 5-ns FWHM), and a fourth harmonic (266 nm, 5-ns FWHM) of Nd:YAG laser (Quanta-Ray; DCR-1A). The second laser (LASER 2) was used in double-flash experiment. The excitation pulsed light was focused on the sample with a 35 cm focal length lens. A probe light source was a pulsed or continuous xenon lamp (300 W, Varian, Xenon illuminator VIX 300 F). The excitation laser beam and probe light beam from the Xe-flash lamp were crossed at the sample position. The light intensity of the xenon-flash lamp was kept constant for 500 μs by the use of light intensity monitor which gives feedback to the power supply of the lamp. An electromagnetic shutter (Copal; EMS No.0) was used to protect samples from being damaged and to avoid the overload current in a photomultiplier. The probe light was selected with a monochromator (Shimadzu-Bausch & Lomb; f=17 cm with 1350 grooves/mm grating) and was detected by a photomultiplier (Hamamatsu Photonics; R666S). The output signal of the photomultiplier was digitized with a transient recorder (Iwatsu; DM901, 9 bits, 10 nsec/point in the fastest writing mode). The digitized signals (1024 points) were analyzed by a microcomputor (NEC, PC8001).

In the measurement both excited and non-excited data were integrated over 4 shots. The sample was stirred before every shot and was exchanged with new sample solution after 20 laser shots.

Double-flash experiment

The excitation light sources of the first and the second flashes were a third harmonic (355 nm, 5-ns FWHM) of a Q-switched Nd:YAG laser (Quanta-Ray; DCR-1A) and a second harmonic (532 nm, 15-ns FWHM) of a Q-switched Nd:YAG laser (Quantel; YG472), respectively. The time interval of the two excitation light pulses was adjusted by a digital delay circuit with a time resolution of 100 ns (ref.19). Figure 1 shows the block diagram of the nanoseconds time-resolved double-flash excitation apparatus. Two excitation beams were precisely adjusted to be coaxial.

RESULTS AND DISCUSSION

Photolysis of $Mn_2(CO)_{10}$ in cyclohexane: Presence of Two Processes

The transient absorption spectrum observed 50 ns after excitation (Fig. 2) (ref.9) is virtually identical with the spectrum of the primary photoproducts in picosecond flash photolysis of $Mn_2(CO)_{10}$ in ethanol (ref.20). The absorption band I with λ_{max} at 827 nm disappears within 30 μs after excitation, while band II with λ_{max} at 500 nm does not decay in the time region. Therefore there are at least two species which show decay kinetics different from each other after being formed by the excitation of $Mn_2(CO)_{10}$. The excitation intensity dependence shows that both species are formed in one-photon processes. Band I is assigned

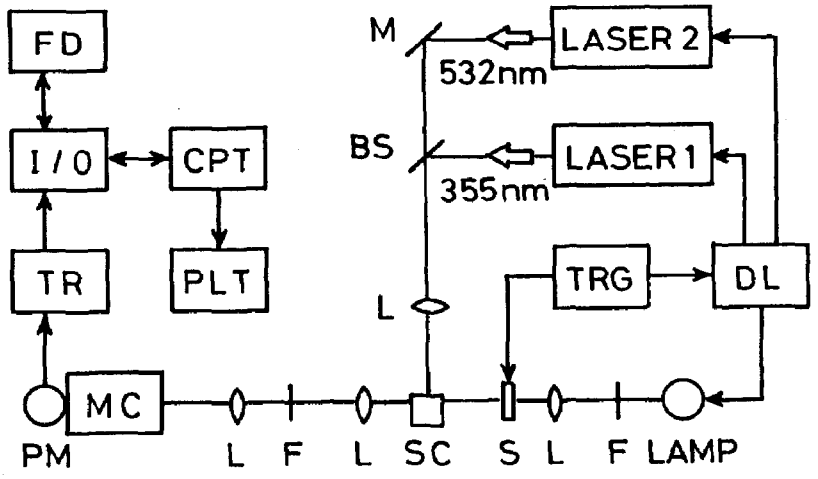

Fig.1. Block diagram of nanosecond time-resolved spectroscopy apparatus. TRG: main trigger circuit, DL: digital delay circuit, BS: beam splitter (355 nm reflection, 532 nm transparence), F: filter, M: mirror, L: lens, S: mechanical shutter, SC: sample cell, MC: monochromator, PM: photomultiplier, TR: transient recorder, I/O: input/output unit, FD: floppy disk driver, CPT: microcomputer, PLT: X-Y plotter.

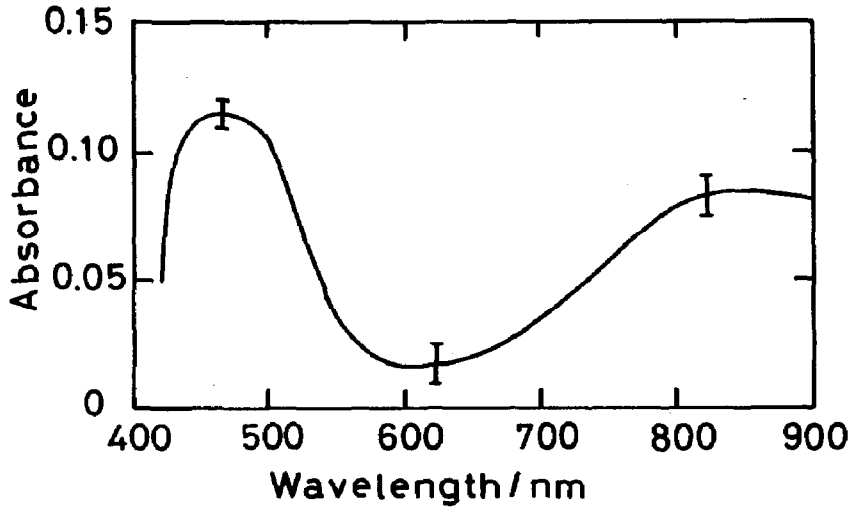

Fig.2. Transient absorption spectrum observed 50 ns after excitation (337 nm) of the cyclohexane solution of $Mn_2(CO)_{10}$.

to the $\cdot Mn(CO)_5$ radical formed by homolysis of the Mn-Mn bond on the basis of the similarity in the absorption spectrum to that of the $\cdot Mn(CO)_5$ radical produced by photolysis of $HMn(CO)_5$ in solid CO matrix by Church et al. (ref.21) and by pulse radiolysis of $Mn_2(CO)_{10}$ in ethanol by Waltz et al. (ref.22) and decay kinetics.

The absorbance at 827 nm of the sample in cyclohexane decreases following the second-order kinetics (see Fig. 3a)(ref.9). This can be interpreted in terms of the recombination reaction of $\cdot Mn(CO)_5$ radicals.

$$2 \cdot Mn(CO)_5 \xrightarrow{k_1} Mn_2(CO)_{10} \qquad [3]$$

$$Mn_2(CO)_9 + L \xrightarrow{k_2} Mn_2(CO)_9L \qquad [4]$$

From the analysis of the plots shown in Fig. 3a, $2k_1/\varepsilon_{827}$ in cyclohexane was defermined at $(2.2\pm0.1)\times10^6$ s^{-1} cm (ref.9), where k_1 is the second-order rate constant for process [3] and ε_{827} represents the molar extinction coefficient of $\cdot Mn(CO)_5$ at 827 nm. The value, $2K_1/\varepsilon_{827}$, in cyclohexane is a little larger than that obtained in ethanol, 1.5×10^6 s^{-1} cm (ref.22). The difference is probably ascribed to the lower viscosity of cyclohexane than ethanol. By using the molar extinction coefficient of $\cdot Mn(CO)_5$ at 830 nm, 800 M^{-1} cm^{-1}, in ethanol (ref.22), the second-order rate constant, k_1, in cyclohexane is estimated to be 8.8×10^8 M^{-1} s^{-1} (ref.9). This is in relatively good agreement with the reported values in cyclohexane, 9.5×10^8 M^{-1} s^{-1} (ref.23) and 1.9×10^9 M^{-1} s^{-1}, and in ethanol, 6.0×10^8 M^{-1} s^{-1} (ref.22).

The absorption band II with λ_{max} at 500 nm can be assigned to another photoproduct, $Mn_2(CO)_9$, which is formed by loss of CO on the basis of the following investigation (vide infra). The absorbance of band II at 500 nm also decreases following the second-order kinetics (Fig. 3b) due to the reaction of $Mn_2(CO)_9$ with CO in equimolar amount. From the analysis of the plot shown in Fig. 3b, k_2/ε_{500} is determined to be $(1.2\pm0.2)\times10^2$ s^{-1} cm (ref.9) where k_2 is the rate constant for disappearance of the species II and ε_{500} represents the molar extinction coefficient of the species II at 500 nm. The same second-order kinetic behavior in the decaying process can be observed at different wavelengths from 500 nm in the spectral region of 430-550 nm. It is emphasized that two transient species corresponding to bands I and II are formed directly by the photoexcitation of $Mn_2(CO)_{10}$ and disappear following the second-order kinetics independent of each other.

The photoexcitation of metal carbonyl compounds often leads to cleavage of metal-CO bond. Only two reports (refs.24,25) made suggestion of the generation of $Mn_2(CO)_9$ by the photoexcitation of $Mn_2(CO)_{10}$ before our direct observation in the previous work (ref.9). It is conceivable that $Mn_2(CO)_9$ is formed by the

excitation of $Mn_2(CO)_{10}$ and that the transient absorption in the shorter wavelength region is due to this intermediate species. $Mn_2(CO)_9$ may be highly reactive with various ligands and $Mn_2(CO)_9(EtCN)$ is known to be a photochemical product between $Mn_2(CO)_{10}$ and EtCN (ref.15). The quenching experiment of species II by EtCN was carried out to investigate the possibility of the assignment of the transient absorption to $Mn_2(CO)_9$.

Photolysis of $Mn_2(CO)_{10}$ in the presence of RCN in cyclohexane: Identification of $Mn_2(CO)_9$

The time dependence of the intensity of the transient absorption at 500 nm induced by the excitation of $Mn_2(CO)_{10}$ solution containing 0.14 M EtCN is shown by curve 1 in Fig. 4. The absorbance decreases to a final value, $A(\infty)$, which is constant over a few seconds. The difference in absorbance between t=t and $t=\infty$, $A(t)-A(\infty)$, decreases exponentially with increasing time (see curve 2 in Fig. 4). This observation indicates that $Mn_2(CO)_9$ reacts with EtCN to form a stable product. The absorption spectrum of the stable product is very close to that of the authentic $Mn_2(CO)_9(EtCN)$. This supports the assignment of the second species as $Mn_2(CO)_9$. In order to estimate the molar extinction coefficient of $Mn_2(CO)_9$, the quenching experiment of $Mn_2(CO)_9$ by MeCN in cyclohexane was carried out. The isosbestic point in the absorption spectra of $Mn_2(CO)_9$ and $Mn_2(CO)_9(MeCN)$ is locatd at 460 mn. Using the molar extinction coefficient of $Mn_2(CO)_9(MeCN)$ at 460 nm (1100 M^{-1} cm^{-1}) and the transient absorption spectrum in Fig. 2, the upper limit of the molar extinction coefficent of $Mn_2(CO)_9$ at 500 nm, ϵ_{500}, is estimated to be 1000 M^{-1} cm^{-1} (ref.9). The rate constant for the reaction of $Mn_2(CO)_9$ with EtCN is determined to be $(4.9\pm0.7)\times10^7$ M^{-1} s^{-1} (ref.9).

The decay in absorbance at 827 nm follows the second-order kinetics with no apparent difference from that in the presence of EtCN showing that $\cdot Mn(CO)_5$ radical does not take part in the formation of $Mn_2(CO)_9(EtCN)$ under the present conditions.

According to the similar quenching experiment by t-BuNC the rate constant for the reaction of $Mn_2(CO)_9$ with t-BuNC was determined to be $(5.4\pm0.5)\times10^7$ M^{-1} s^{-1} (ref.9). The rate constant for the reaction of $Mn_2(CO)_9$ with CO in cyclohexane is calculated as 1.2×10^5 M^{-1} s^{-1} (ref.9). The reactivity of $Mn_2(CO)_9$ is higher with EtCN than with CO. This fact is consistent with the previous report that the rate constant (1.6×10^8 M^{-1} s^{-1}) (ref.26) of the reaction of CH_3CN with $Cr(CO)_5$ in cyclohexane is much larger than that of CO with $Cr(CO)_5$ (3×10^6 M^{-1} s^{-1}) (ref.27).

By using these estimated values, together with the optical path length of our system (0.7 cm), and the transient absorption spectrum in Fig. 2, the

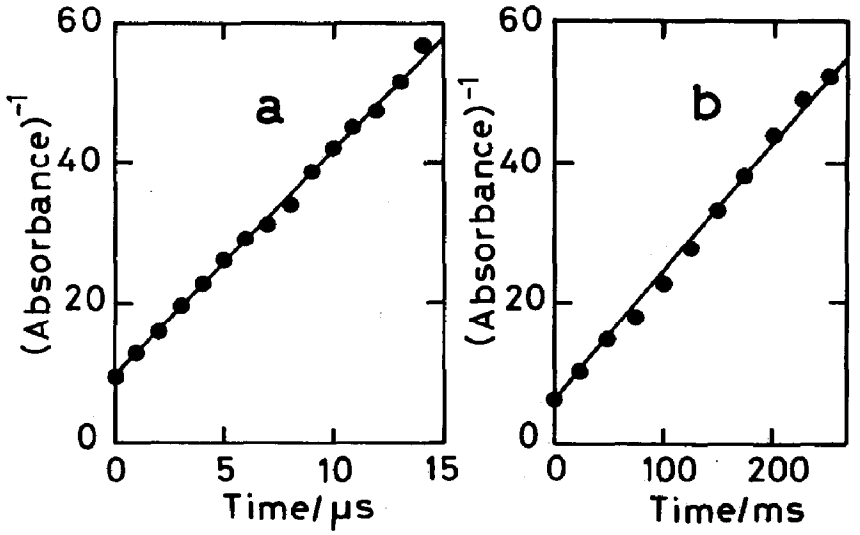

Fig.3. Second-order kinetic plots of transients in the cyclohexane solution of $Mn_2(CO)_{10}$: a. 827 nm; b. 500 nm.

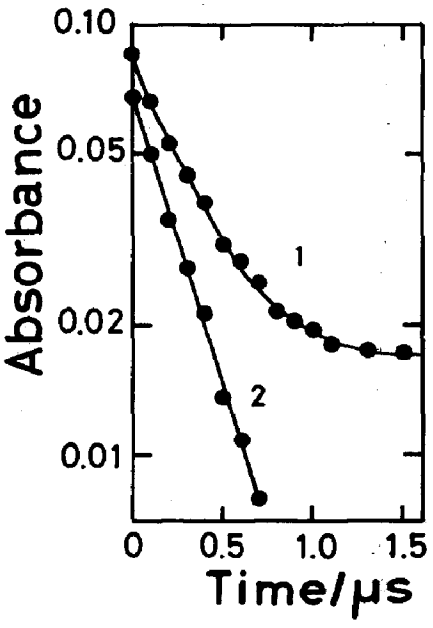

Fig.4. Time dependence of absorbance at 500 nm in the presence of 0.14 M of EtCN: curve 1, observed time profile; curve 2, $A(t)-A(\infty)$ where $A(\infty)$ is the average absorbance at a delay time longer than 1.5 μs.

concentrations of $\cdot Mn(CO)_5$ and $Mn_2(CO)_9$ 50 ns after excitation are estimated to be 1.5×10^{-4} M and $\gtrsim1.4\times10^{-4}$ M, respectively (ref.9). The concentrations of both $\cdot Mn(CO)_5$ and $Mn_2(CO)_9$ are almost one-third of the concentration of $Mn_2(CO)_{10}$ in a sample. This means that the quantum yields for the formation of $\cdot Mn(CO)_5$ and $Mn_2(CO)_9$ are equal to or larger than 0.3. Therefore in the photochemical reaction of $Mn_2(CO)_{10}$ the cleavage of the Mn-CO bond is as important as the Mn-Mn bond fission.

Photolysis of $Mn_2(CO)_{10}$ in the presence of $P(n\text{-}Bu)_3$ in cyclohexane: Reactivity of the Two Transients toward PBu_3

Though the photolysis in the presence of $P(n\text{-}Bu)_3$ is complicated, there are two distinct features in the time dependence of transient absorption observed in the system. One feature is the rapid increase in absorbance at 475 nm when the concentration of the phosphine is 2.0×10^{-3} M as is shown by the curve 1 in Fig. 5 (ref.9). The absorbance increases to a final value 2 μs after excitation. The absorbance difference, $A(\infty)-A(t)$, obeys the first-order kinetics (see the curve 2 in Fig. 5). In the wavelength region 525–550 nm the absorbance decreases and approaches to a constant final value around 2 μs after excitation. These observations indicate that the increase in absorbance at 475 nm is due to the reaction of $Mn_2(CO)_9$ with $P(n\text{-}Bu)_3$. The rate constant for the reaction of $Mn_2(CO)_9$ with $P(n\text{-}Bu)_3$ is determined to be $(1.0\pm0.1)\times10^9$ M^{-1} s^{-1} (ref.9).

The decay curve of the transient absorption at 827 nm for the solution containing 2.0×10^{-3} M of $P(n\text{-}Bu)_3$ is shown by the curve 1 in Fig. 6 (ref.9). Comparison of the curve with the curve 1 in Fig. 5 leads to the conclusion that there is no correlation between the formation of $Mn_2(CO)_9[P(n\text{-}Bu)_3]$ and the decay of $\cdot Mn(CO)_5$. This means that the replacement of CO of $\cdot Mn(CO)_5$ by $P(n\text{-}Bu)_3$ does not occur appreciably at the lower phosphine concentration.

The other feature is the time dependence of absorbance at 827 nm and 450 nm for the solution containing 2.0×10^{-2} M of $P(n\text{-}Bu)_3$ which are shown by the curves 2 and 3, respectively, in Fig. 6. The absorbance at 827 nm decreases with time, while that at 450 nm increases. Later than 2 μs after excitation both the absorbances at 827 nm and at 450 nm follow the second-order kinetics (ref.27). $Mn_2(CO)_8[P(n\text{-}Bu)_3]_2$ possesses its absorption bands in the wavelength region shorter than 550 nm (ref.28). These facts indicate that the replacement of CO of $\cdot Mn(CO)_5$ by $P(n\text{-}Bu)_3$ occurs at higher phosphine concentration and the substituted radicals, $\cdot Mn(CO)_4[P(n\text{-}Bu)_3]$, recombine to form $Mn_2(CO)_8[P(n\text{-}Bu)_3]_2$ molecules. In order to identify the products from the photolysis in the presence of $P(n\text{-}Bu)_3$, they were accumulated by the exposure of 100 laser shots on one sample of $Mn_2(CO)_{10}$ (3×10^{-4} M) and $P(n\text{-}Bu)_3$ (1×10^{-2} M) and $Mn_2(CO)_9[P(n\text{-}Bu)_3]$ and $Mn_2(CO)_8[P(n\text{-}Bu)_3]_2$ were identified by ordinary IR method. The products ratio at about 10 % conversion was found to be 1:3.

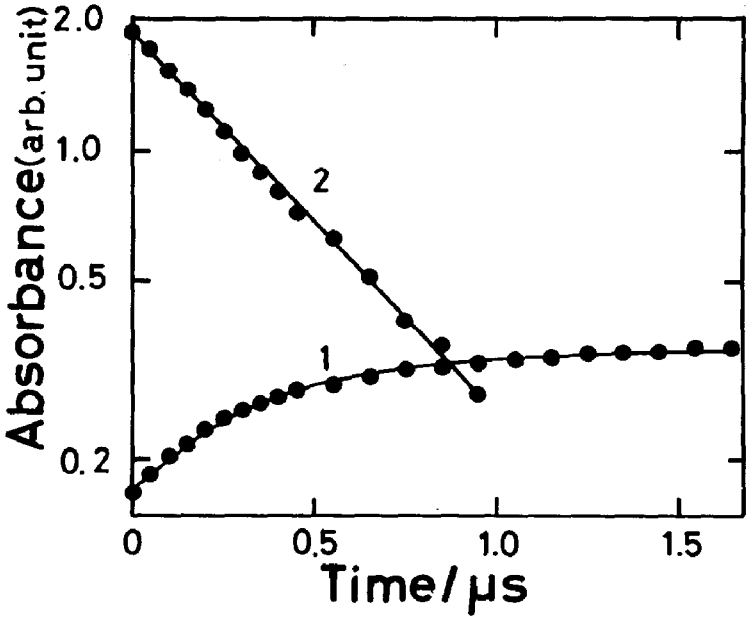

Fig.5. Time dependence of absorbance at 475 nm in the presence of 2.0×10^{-3} M of $P(n\text{-}Bu)_3$: curve 1, observed time profile; curve 2, $A(\infty)-A(t)$.

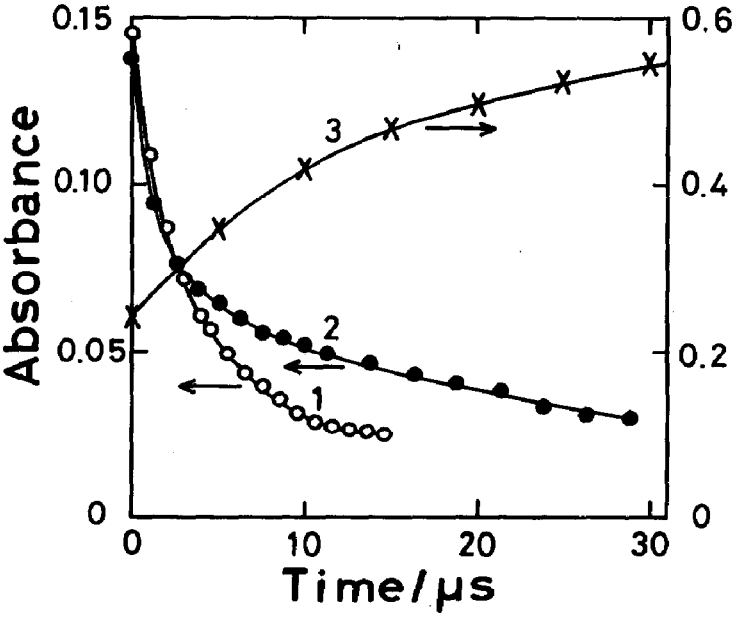

Fig.6. Time dependence of absorbance in the presence of $P(n\text{-}Bu)_3$: curve 1, 827 nm, $[P(n\text{-}Bu)_3]=2.0\times10^{-3}$ M; curve 2, 827 nm, $[P(n\text{-}Bu)_3]=2.0\times10^{-2}$ M; curve 3, 450 nm, $[P(n\text{-}Bu)_3]=2.0\times10^{-2}$ M.

Since the work by Kidd and Brown (ref.17) on the photochemical substitution of $Mn_2(CO)_{10}$ with $P(n\text{-}Bu)_3$, it has been widely accepted that the 17-electron metal-centered carbonyl species undergo facile dissociative loss of CO. However, the controversy (ref.29) whether $\cdot Mn(CO)_5$ is dissociative or associative on the displacement of CO ligands is now clarified as mentioned above by our present study. The observed difference in the decaying kinetics of the radical between lower and higher phosphine concentration and no interaction of CH_3CN with the radical (vide supra) clearly show that $\cdot Mn(CO)_5$ radicals do not undergo facile dissociative loss of CO and the substitution of CO by $P(n\text{-}Bu)_3$ proceeds through an associative process under the experimental conditions. This feature of $\cdot Mn(CO)_5$ substitution reaction has been also observed by the low temperature matrix technique (ref.12). The closely related reaction of $\cdot Re(CO)_5$ with PPh_3 has been reported to be associative in the photochemical competition reaction with CCl_4 by Fox et al. (ref.30) and also the associative nature of the substitution of $\cdot Mn(CO)_3[P\text{-}(n\text{-}Bu)_3]_2$ with CO has been shown by McCullen et al. (ref.31).

Photolyses of $Mn_2(CO)_{10}$ in CCl_4 and in $CHCl_3$

The transient absorption intensity at 827 nm decreases obeying the first-order kinetics as shown in Fig. 7 (refs.9,32a). This means that the reaction of the $\cdot Mn(CO)_5$ radical with CCl_4 is faster than the recombination reaction of $\cdot Mn(CO)_5$ radicals under our experimental conditions. The rate constant is determined to be $(9.1\pm0.8)\times10^5$ s^{-1} in the previous paper (refs.32a,33). The decay of $Mn_2(CO)_9$ also follows the first-order kinetics, and the rate constant is determined to be $(2.1\pm0.4)\times10^2$ s^{-1} (ref.9). This observed kinetics can be interpreted in terms of the reaction of $Mn_2(CO)_9$ with CCl_4 and/or $\cdot CCl_3$ radical formed by the reaction of the $\cdot Mn(CO)_5$ radical with CCl_4. The increase in absorbance in the spectral region 430-500 nm is observed after the disapperance of $Mn_2(CO)_9$. Although the explanation for this observation is not yet clear, noteworthy is the generation of $Mn_2(CO)_9$ even in CCl_4 also supporting non-radical nature of its origin.

The decay of the transient absorption intensity at 827 nm observed for $Mn_2(CO)_{10}$ in $CHCl_3$ obeys the second-order kinetics. Therefore the reaction rate of the $\cdot Mn(CO)_5$ radical with $CHCl_3$ is much smaller than the recombination rate of $\cdot Mn(CO)_5$ radicals. This is consistent with the report that the reaction rate costant of CCl_4 to the metal radical ($(\eta^5\text{-}C_5H_5)W(CO)_3$) is larger than that of $CHCl_3$ by three orders of magnitude (ref.34).

Excitation wavelength dependence on the photodissociation of the two processes in $Mn_2(CO)_{10}$

Figure 8 shows the transient difference absorption spectra of $Mn_2(CO)_{10}$ in

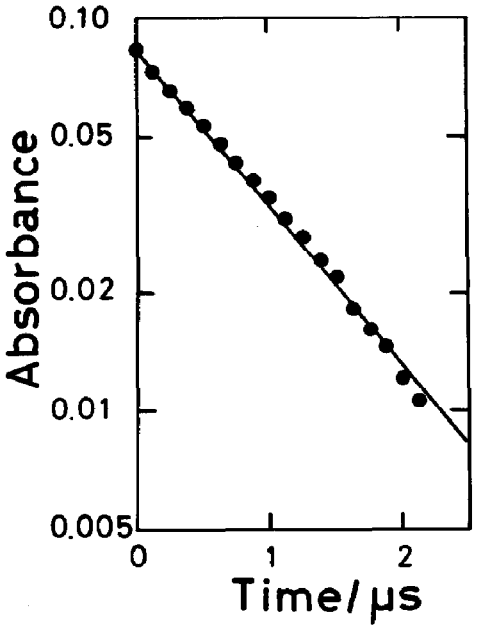

Fig.7. First-order kinetic plot for decay of transient at 827 nm in CCl_4 solution of $Mn_2(CO)_{10}$.

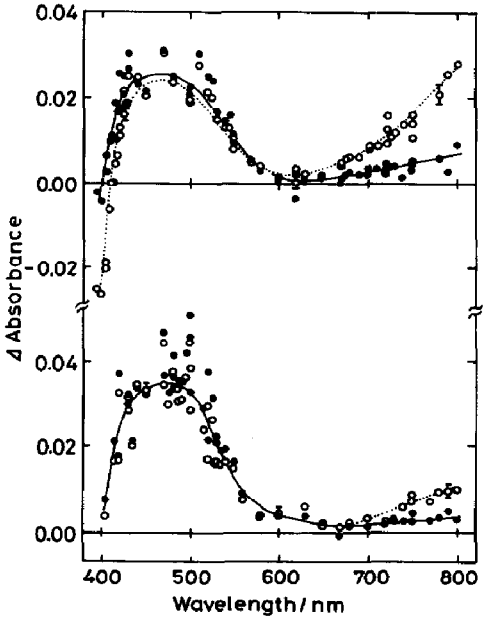

Fig.8. Transient difference absorption spectra of $Mn_2(CO)_{10}$ in cyclohexane excited by 355 nm (top) and by 266 nm pulse (bottom) observed 3 μs (open circles) and 30 μs (closed circles) after excitation.

cyclohexane following 355 nm (top) and 266 nm (bottom) excitations. The absorbance with λ_{max} at 800 nm is due to $\cdot Mn(CO)_5$ radical which decays in the recombination process [3]. The second-order rate constant, k_1, in cyclohexane is estimated for both 266 and 355 nm excitations to be 8.5×10^8 M^{-1} s^{-1}, which is very close to the previously reported value for the 337 nm excitation (8.8×10^8 M^{-1} s^{-1}) (ref.9). The absorbance at 500 nm is due to $Mn_2(CO)_9$ (ref.9) and the second-order rate constant for the reaction of $Mn_2(CO)_9$ with CO has been estimated to be in the order of 10^{5-6} M^{-1} s^{-1} (refs.9-11). Since the photogenerated $Mn_2(CO)_9$ and $\cdot Mn(CO)_5$ do not disappear appreciably in 30 ns after excitation, the present nanosecond experiment allows the direct real-time observation of the initial amount of both primary photoproducts under the conditions without the subsequent bimolecular recombination of $\cdot Mn(CO)_5$ and/or a probable secondary photoreaction of $Mn_2(CO)_9$ (ref.35). The quantum yield ratio of the processes [1] and [2], Y_1/Y_2, is estimated from the absorbance ratio, R, at 800 nm over 500 nm just after excitation as follows:

$$R = A(800\ nm)/A(500\ nm) = 2Y_1\varepsilon_{800}/\ Y_2\varepsilon_{500}$$

For the calculation of R, the absorbances at 800 and 500 nm averaged over 0-30 ns after excitation are used. From the reported spectral shapes (refs.9,22) and the values of $\varepsilon_{500} \sim 1000$ M^{-1} cm^{-1} (ref.9), $\varepsilon_{510} = 800 \pm 300$ M^{-1} cm^{-1} (ref.11) and $\varepsilon_{830} = 800 \pm 80$ M^{-1} cm^{-1} (ref.22), $\varepsilon_{830} = 950$ M^{-1} cm^{-1} (ref.36), the ratio, $\varepsilon_{830}/\varepsilon_{500}$, can be estimated at about unity.

The value, $Y_1/Y_2 = R/2$, thus estimated increases with the excitation wavelength as shown in Table 1. The electronic absorption spectrum of $Mn_2(CO)_{10}$ has been assigned as follows: 374 nm ($d\pi-\sigma^*$), 336 nm ($\sigma-\sigma^*$), 303 nm ($\sigma-\pi^*$), and 266 nm ($d\pi-\pi^*$) (ref.4). This clearly shows that the rate of the internal conversion is smaller than the reaction rate. The value, Y_1/Y_2, shows that in the case of the $d\pi \rightarrow \pi^*$ excitation, M-CO cleavages are more efficient than M-M fissions by a factor of five. It is worth to mention that the CO cleavage is slightly more efficient than the radical formation (ref.37) even by the lower energy σ^* excitation. Both $\sigma \rightarrow \sigma^*$ excitation and $d\pi \rightarrow \pi^*$ excitation have reaction channels to [1] and [2]. However it should be also noted that the photoirradiation induces the direct fission of the metal-metal bond without M-CO cleavage. This is in contrast with the thermal reaction in which the absence of metal-metal bond cleavage has lately been verified (ref.35a).

Photolysis of $Re_2(CO)_{10}$ in cyclohexane

Upon excitation with 355 nm laser pulse, an argon filled cyclohexane solution of $Re_2(CO)_{10}$ showed a transient spectrum which was revealed to consist of two components as shown in Fig. 9. One absorption with λ_{max} at around 550 nm, which

TABLE 1

The dependence of the relative ratio, Y_1/Y_2 on the excitation wavelength λ_e.

λ_e/nm	solvent	Δt^c	Y_1/Y_2
266	cyclohexane	5 ns	0.21 ± 0.07
337[a]	cyclohexane	10 ns	0.37 ± 0.05
347[b]	ethanol	25 ps	~ 0.43
355	cyclohexane	5 ns	0.74 ± 0.15

a) Reference 9.

b) Reference 20.

c) Excitation pulse width (FWHM).

disappears within 20 μs, is piled on another absorption with λ_{max} at 420 nm which tails off over 600 nm.

The absorption (λ_{max} 550 nm) is attrributed to $\cdot Re(CO)_5$ on the bases of the absorption spectrum, its decay kinetics, and quenching with CCl_4 in literature (ref.32a). The decay of the absorbance at 500 nm follows the second-order kinetics as shown in Fig. 10, which gives the observed value, $k_3/\varepsilon_{500}\,\ell_{eff} = (1.5\pm0.2)\times10^7\ s^{-1}$: k_3 is the rate constant for the recombination reaction [5], ε_{500} represents the molar extinction coefficient at 500 nm, and ℓ_{eff} is the effective path length.

$$2\ \cdot Re(CO)_5 \xrightarrow{k_3} Re_2\ (CO)_{10} \qquad [5]$$

By using the reported value, $\varepsilon_{500} = 800\ M^{-1}\ cm^{-1}$ in ethanol (ref.32a), the value of k_3 is determined to be $(3.6\pm0.5)\times10^9\ M^{-1}\ s^{-1}$. This is in good agreement with the reported values of $3.7\times10^9\ M^{-1}\ s^{-1}$ in hexane (ref.23) and $5.4\times10^9\ M^{-1}\ s^{-1}$ in ethanol (ref.32a).

When CCl_4 (1.67×10^{-2} M) is added, the decay becomes faster and follows a pseudo-first-order kinetics. The rate constant for the reaction of $\cdot Re(CO)_5$ with CCl_4 is estimated to be $5.8\times10^7\ M^{-1}\ s^{-1}$. This is nearly equal to the reported value, $3.9\times10^7\ M^{-1}\ s^{-1}$, in ethanol (ref.32a).

The other absorption with λ_{max} at 420 nm has a longer lifetime ($\tau\sim30$ ms) under 1 atm. of Ar and the decay of the absorbance at 430 nm follows the second-order kinetics as shown in Fig. 11a. From which a value, $k_4/\varepsilon_{430}\,\ell_{eff} = (1.2\pm0.5)\times10^3\ s^{-1}$, was obtained: k_4 is the rate constant for the reaction of the second intermediate with eliminated CO. When 1 atm. of CO is admitted, the

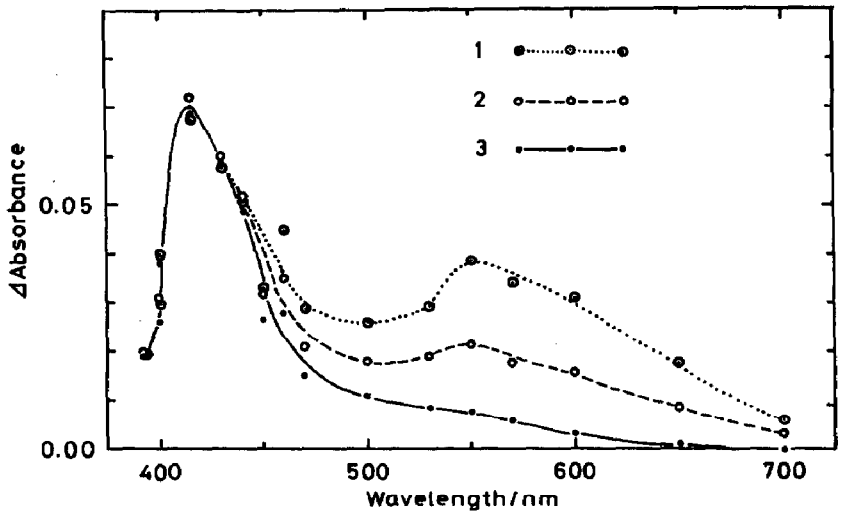

Fig.9. Transient difference absorption spectra of $Re_2(CO)_{10}$ in cyclohexane following 355 nm excitation. Delay times are 0.5, 3, and 30 μs for curves 1-3, respectively.

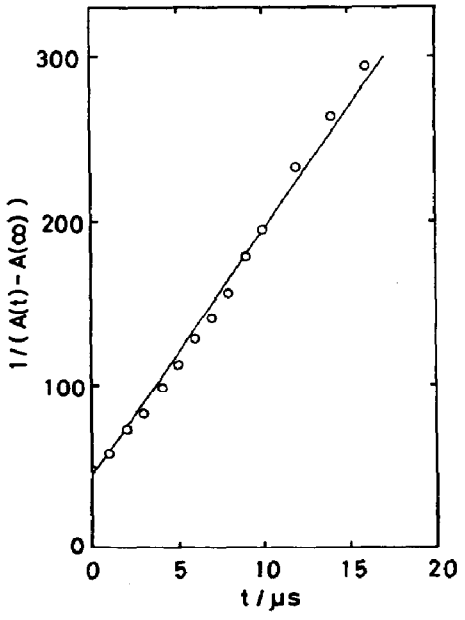

Fig.10. Time dependence of absorbance of $Re_2(CO)_{10}$ in cyclohexane at 500 nm after excitation at 355 nm. Inverse of absorbance $[A(t)-A(\infty)]^{-1}$ versus delay time for the sample solution under 1 atm. of Ar.

decay of the absorbance at 430 nm increases and follows the pseudo-first-order kinetics as shown in Fig. 11b, whereas the addition of CCl_4 to the Ar filled system does not affect the absorbance change and the decay rate of the second absorption. These facts clearly show that the second transient absorption can be attributed to the formation of a dirhenium species of CO unsaturation via a non-radical path similar to the CO dissociation process of $Mn_2(CO)_{10}$ system. From the observed pseudo-first-order rate constant, $k'_{obs(430)} = (4.4\pm0.4)\times10^2$ s^{-1}, the second-order rate constant for the reaction [6] is estimated as $k_4 = 4.4\times10^4$ M^{-1} s^{-1} by assuming the concentration of CO to be 1×10^{-2} M in cyclohexane at 1 atm. of CO pressure (ref.38).

$$Re_2(CO)_{10-n} + n\ CO \xrightarrow{k_4} Re_2(CO)_{10} \qquad [6]$$

The recombination rate constant of the second transient of rhenium with CO is one order of magnitude smaller than that of $Mn_2(CO)_9$, 4.2×10^5 M^{-1} s^{-1} which is determined by the same method (ref.39).

By using the estimated k_4 value, the value ε_{430} is evaluated at 400 ± 150 M^{-1} cm^{-1} from $k_4/\varepsilon_{430}\,l_{eff}$. The quantum yield ratio between the two reaction processes, Y_1/Y_2, can be estimated at 0.15 at 355 nm excitation based on the estimated ε_{430} and ε_{500} in the previous paper (ref.32a). The Y_1/Y_2 value for $Re_2(CO)_{10}$ indicates that the CO dissociation process is much a more dominant process over the homolysis of metal-metal bond compared with $Mn_2(CO)_{10}$ system in which Y_1/Y_2 at 355 nm excitation is 0.75 (see table).

Double-flash excitation

Figure 12 shows the kinetics of the transient absorption of $Mn_2(CO)_{10}$ in cyclohexane at 500 nm. $Mn_2(CO)_9$ is formed just after 355 nm excitation (see curve 2 in Fig. 12). The transient absorption intensity decreases when the second pulse (532 nm) is irradiated on the sample 30 μs after the first pulse (355 nm) (see curve 1). The recovery of the transient absorption is not found within 60 μs after the second pulse excitation. No signal is observed when the sample is irradiated only by the second pulse (see curve 3). Figure 12 clearly shows that the photochemical reaction of $Mn_2(CO)_9$ is caused by the second pulse. On the analogy of the photoreaction of $Mn_2(CO)_{10}$, there are two possible processes as follows.

$$Mn_2(CO)_9 \xrightarrow{532\ nm} \bullet Mn(CO)_5 + \bullet Mn(CO)_4 \qquad [7]$$

$$Mn_2(CO)_9 \xrightarrow{532\ nm} Mn_2(CO)_8 + CO \qquad [8]$$

Figure 13 shows the kinetics of the transient absorption of $Mn_2(CO)_{10}$ at 780 nm. If the cleavage of Mn-Mn bond takes place $\bullet Mn(CO)_5$ radical is to be formed (process [7]) (ref.35a). However no detectable signal was observed at 780 nm

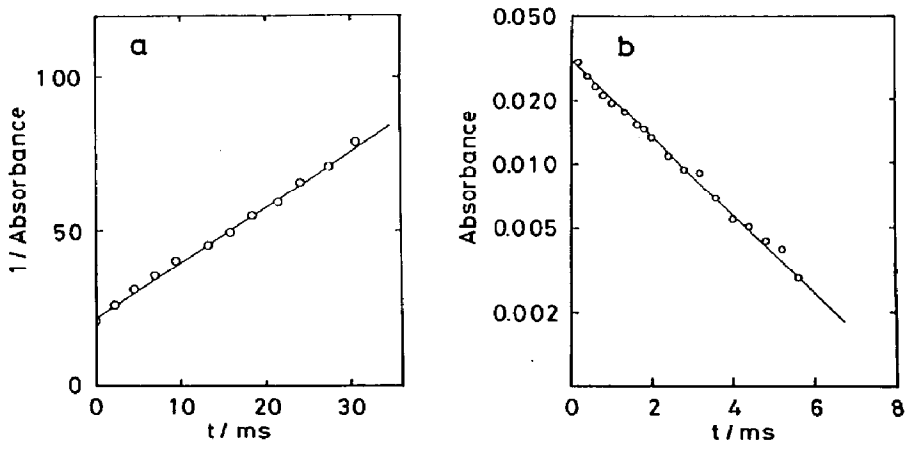

Fig.11. Time dependence of absorbance change of $Re_2(CO)_{10}$ in cyclohexane at 430 nm after the excitation at 355 nm. (a) Inverse of absorbance versus delay time for the sample solution under 1 atm. of Ar; (b) Absorbance versus delay time for the solution under 1 atm. of CO.

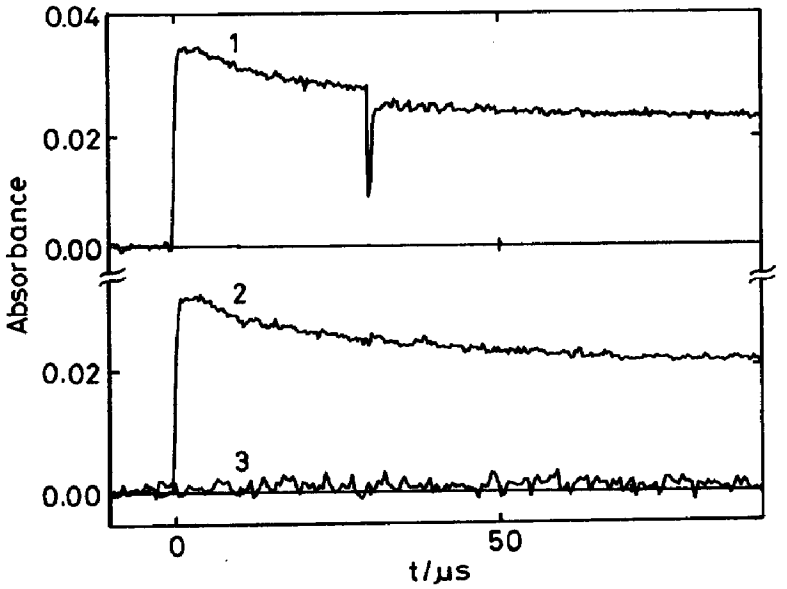

Fig.12. Kinetics of the transient absorption of $Mn_2(CO)_{10}$ in cyclohexane at 500 nm. Curve 1, double flash; curve 2, 355 nm flash; curve 3, 532 nm flash.

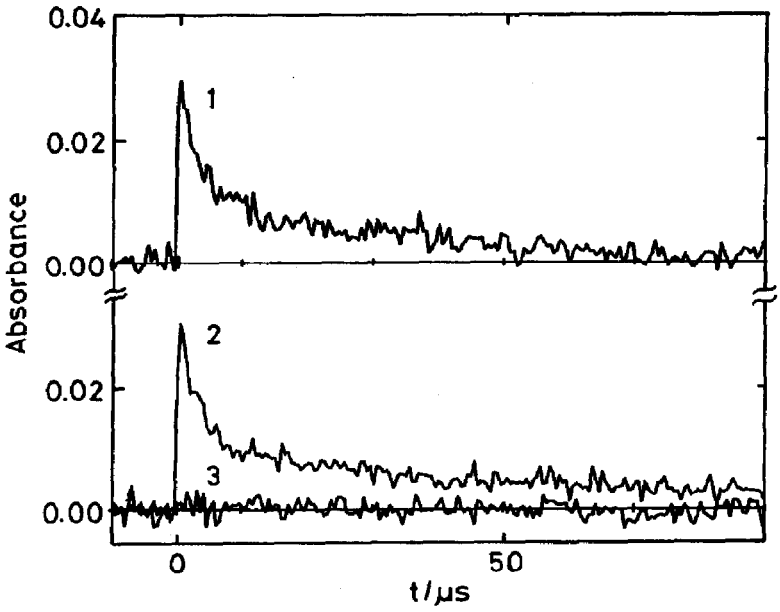

Fig.13. Kinetics of the transient absorption of $Mn_2(CO)_{10}$ in cyclohexane at 780 nm. Curve 1, double flash; curve 2, 355 nm flash; curve 3, 532 nm flash.

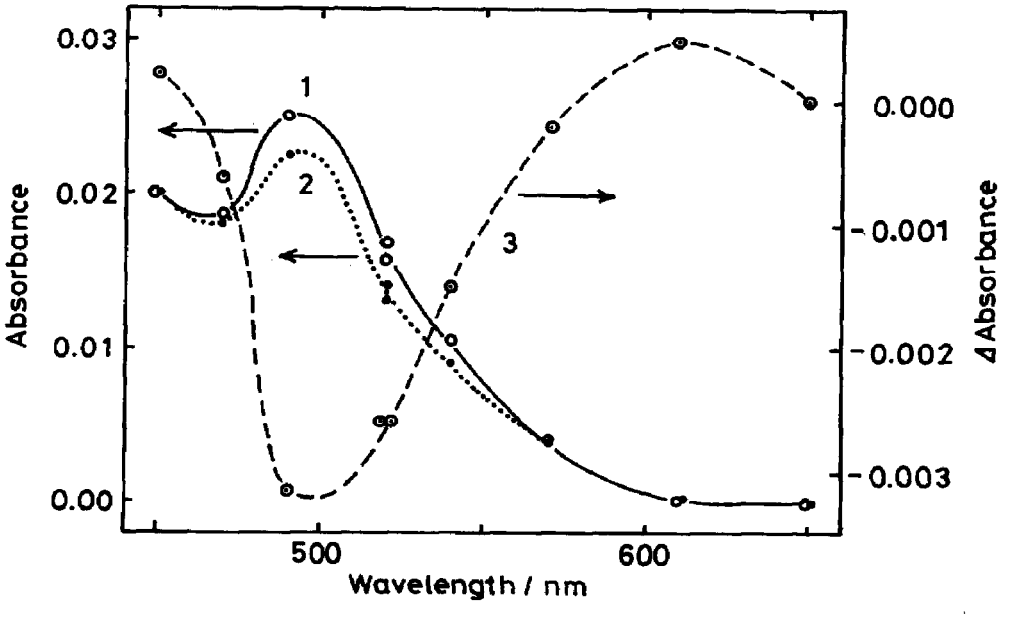

Fig.14. Transient difference absorption spectra of $Mn_2(CO)_{10}$ in cyclohexane following 355 nm excitation. Curve 1; 5 μs before the second pulse (532 nm) excitation, curve 2; 3 μs after the second pulse excitation, curve 3; difference spectrum between curves 1 and 2.

where the molar extinction coefficient of $\cdot Mn(CO)_5$ is nearly equal to that of $Mn_2(CO)_9$. The yield of process [7] is therefore concluded to be low. The major process is not the cleavage of Mn-Mn bond but of Mn-CO bond (process [8]). Curve 3 in Fig. 14 shows the difference absorption spectra between 5 μs before (curve 1) and 3 μs after (curve 2) the second pulse excitation. The decrease in the absorbance around 500 nm is caused by the disappearance of $Mn_2(CO)_9$. The experiments of CO effect on the kinetics of the transient absorption and of steady-state irradiation at low temperature are in progress to clarify the products of photoreaction of $Mn_2(CO)_9$.

The excitation wavelength dependence of the braching ratio of processes [1] and [2], the double-flash experiment, and the photolysis of the rhenium system will be published elsewhere.

REFERENCES AND NOTES

1 M. S. Wrighton and G. L. Geoffroy, Organometallic Photochemistry, Academic Press, New York, 1978.
2 G. L. Geoffroy, J. Chem. Educ., 60 (1983) 861.
3 M. S. Wrighton and D. S. Ginley, J. Am. Chem. Soc., 97 (1975) 2065.
4 R. A. Levenson and H. B. Gray, J. Am. Chem. Soc., 97 (1975) 6042.
5 A. S. Stiegman and D. R. Tyler, Acc. Chem. Res., 17 (1984) 61.
6 D. R. Tyler, M. A. Schmidt, and H. B. Gray, J. Am. Chem. Soc., 101 (1979) 2753; ibid., 105 (1983) 6018.
7 J. V. Caspar and T. J. Meyer, J. Am. Chem. Soc., 102 (1980) 7794.
8 B. D. Moore, M. B. Simpson, M. Poliakoff and J. J. Turner, J. Chem. Soc., Chem. Commun., (1984) 972.
9 H. Yesaka, T. Kobayahsi, K. Yasufuku, and S. Nagakura, Reza Kagaku Kenkyu, 3 (1981) 97; J. Am. Chem. Soc., 105 (1983) 6249.
10 S. P. Church, H. Herman, F. -W. Grevels, and K. Schaffner, J. Chem. Soc., Chem. Commun., (1984) 785.
11 R. S. Herrick and T. L. Brown, Private communication.
12 A. F. Hepp and M. S. Wrighton, J. Am. Chem. Soc., 105 (1983) 5934.
13 R. B. King, J. C. Stokes, and T. F. Korenowski, J. Organomet. Chem., 11 (1968) 641.
14 U. Koelle, J. Organomet. Chem., 155 (1978) 53.
15 M. L. Ziegler, H. Haas, and R. K. Sheline, Chem. Ber., 98 (1965) 2454.
16 G. H. Jeffery and A. I. Vogel, J. Chem. Soc., (1948) 679.
17 R. D. Kidd and T. L. Brown, J. Am. Chem. Soc., 100 (1978) 4095.
18 I. Ugi and R. Mayr, Chem. Ber., 93 (1960) 239.
19 T. Kobayashi and S. Koshihara, Chem. Phys, Lett., 104 (1984) 174.
20 L. J. Rothberg, N. J. Cooper, K. S. Peters and V. Vaida, J. Am. Chem. Soc., 104, (1982) 3536.
21 S. P. Church, M. Poliakoff, J. A. Timney and J. J. Turner, J. Am. Chem. Soc., 103 (1981) 7515.
22 W. L. Waltz, O. Hackelberg, L. M. Dorfman and A. Wojcicki, J. Chem. Soc., 100 (1978) 7259.
23 R. W. Wegman, R. J. Olsen, D. R. Gard, L. R. Faulkner and T. L. Brown, J. Am. Chem. Soc., 103 (1981) 6089.
24 J. L. Hughey IV, C. P. Anderson and T. J. Meyer, J. Organomet. Chem., 125 (1977) C49.
25 A. Fox and A. Poe, J. Am. Chem. Soc., 102 (1980) 2497.
26 J. M. Kelly, D. V. Bent, H. Hermann, D. Schulte-Frohlinde, and E. Koerner von Gustorf, J. Organomet. Chem., 69 (1974) 259.

27 J. M. Kelly, H. Hermann, and E. Koerner von Gustorf, J. Chem. Soc., Chem. Commun., (1973) 105.
28 R. A. Jackson and A. Poë, Inorg. Chem., 17 (1978) 997.
29 A. Poë, Transition Met. Chem. (Weinheim, Ger), 7 (1982) 65 and references therein.
30 A. Fox, J. Malito, and A. Poë, J. Chem. Soc., Chem. Commun., (1981) 1052.
31 S. B. McCullen, H. W. Walker, and T. L. Brown, J. Am. Chem. Soc., 104 (1982) 4007.
32 Reported value for the pseudo-first-order rate consant for $\cdot Mn(CO)_5$ with CCl_4 in ethanol, $(6.1\pm0.8)\times10^5$ M^{-1} s^{-1} (ref.32a).
a) K. W. Meckstroth, R. T. Walters, W. L. Waltz, A. Wojcicki, and L. M. Dorfman, J. Am. Chem. Soc., 104 (1982) 1842.
33 Because the molar extinction coefficient of $Mn(CO)_5Cl$ is very small in wavelengths longer than 400 nm (ref.33a), the increase in absorbance in that region could not be observed.
a) C. H. Bamford, J. W. Burley, and M. Coldbeck, J. Chem. Soc. Dalton Trans, (1972) 1846.
34 R.M. Laine and P.C. Ford, Inorg.Chem., 16 (1977) 388.
35 The experiment of excitation by pulses longer than 1 μs or by ordinary light sources will be suffered from a possible subsequent reaction following the CO cleavage [2] as follows (ref.35a):
$Mn_2(CO)_9 \longrightarrow \cdot Mn(CO)_5 + \cdot Mn(CO)_4$
a) N. J. Coville, A. M. Stolzenberg, E. L. Muetterties, J. Am. Chem. Soc., 105 (1983) 2499.
36 H. W. Walker, R. S. Herrick, R. J. Olsen, and T. L. Brown, Private communication.
37 A different value of Y_1/Y_2 (about 2) was estimated by the competition reaction method (ref.12) and a flash photolysis with 35 μs pulse (ref.11). We consider that their experiments (refs.11,12) may be suffered from complications due to the stationary or longer pulse excitation by polychromatic lamps of which spectrum extends to longer wavelength region.
38 E. Wilhelm and R. Battino, Chem. Rev., 73 (1973) 1.
39 K. Yasufuku, H. Noda, J. Iwai, H. Ohtani, and T. Kobayashi, Sci. Papers I.P.C.R., 78 (1984) in press.